

m²/g; 120 min, 1.00 m²/g; 240 min, 0.57 m²/g; with errors of $\pm 5\%$.

Scanning electron micrographs were obtained on Ni samples irradiated for 0, 15, and 120 min, as shown in Figure 2. As the malleable particles are irradiated, profound changes in particle aggregation and morphology are observed. The surface of our Ni powder is initially highly crystalline, but upon sonication the surface is smoothed quite rapidly. At the same time, the extent of aggregation increases dramatically. We believe that both effects are due to interparticle collisions driven by the turbulent flow created by the ultrasonic field. The increase aggregation accounts for the eventual decrease in the observed surface area and probably also causes the small diminution in activity observed after lengthy sonication.

This change in surface morphology is associated with a dramatic change in surface composition. Auger electron spectra depth profiles were obtained on Ni samples before and after sonication, as shown in Figure 3. Initially, a thick oxide coat is found (with a surface Ni/O ratio of 1.0) extending ≈ 250 Å into the particle. After 1 h of ultrasonic irradiation in octane, the oxide layer is much thinner (< 50 Å, with a surface Ni/O ratio of 2.0). In fact, most of the oxide layer in the irradiated sample is due to its air exposure during sample transfer; the oxide coating is fully reestablished after ≈ 15 min of air exposure. It is likely that the origin of our observed sonocatalytic activity comes from the removal (through interparticle collisions) of the surface oxide layer normally found on Ni powders. A clean Ni surface is an active catalyst;¹³ nickel powder with its usual surface oxide coating is not.

Acknowledgment. Special thanks are due Dr. Frank Scheltens for assistance with the scanning electron micrographs and Nancy Finnegan for the Auger electron spectra; both analyses were carried out in the Center for Microanalysis of Materials, University of Illinois, which is supported by the U.S. Department of Energy under Contract DE-AC 02-76ER 01198. We also thank Brian Borglum and Professor R. C. Buchanan for their aid in obtaining surface area measurements. The support of the National Science Foundation (CHE 8319929) is greatly appreciated. K.S.S. gratefully acknowledges the receipt of an N.I.H. Research Career Development Award and of a Sloan Foundation Research Fellowship.

Esperamicins, a Novel Class of Potent Antitumor Antibiotics. 2. Structure of Esperamicin X

Jerzy Golik,^{*1a} Jon Clardy,^{1b} George Dubay,^{1a}
Gary Groenewold,^{1a} Hiroshi Kawaguchi,^{1c}
Masataka Konishi,^{1c} Bala Krishnan,^{1a} Hiroaki Ohkuma,^{1c}
Kyo-ichiro Saitoh,^{1c} and Terrence W. Doyle^{1a}

Bristol-Myers Pharmaceutical
Research and Development Division
Wallingford, Connecticut 06492
Department of Chemistry, Cornell University
Ithaca, New York 14853
Bristol-Myers Research Institute
Tokyo Meguro, Tokyo, Japan
Received November 28, 1986

Recently we have described the isolation and partial structure elucidation of esperamicins A₁ and A₂ which are produced by cultures of *Actinomadura verrucosospora* (BBM1675, ATCC 39334)^{2,3a,b} and are characterized by broad spectrum antitumor

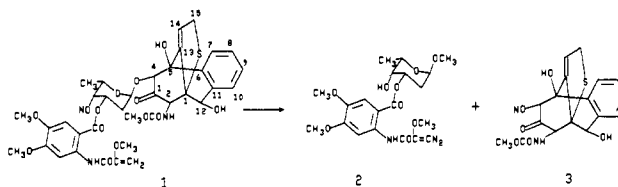


Figure 1. Methanolysis of esperamicin X—stereochemistry of tetracyclic core arbitrarily chosen.

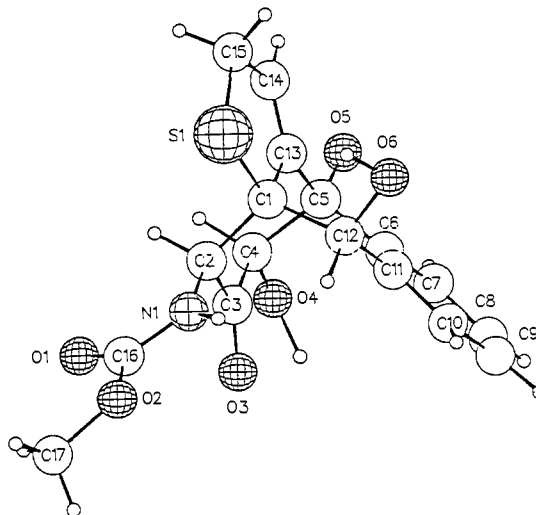


Figure 2. Computer-generated perspective drawing of 3.

activity in murine systems.⁴ To our knowledge they are the most potent antitumor agents yet discovered. The esperamicins are produced as a complex of related compounds which we have resolved into a number of components, A₁, A₂, A_{1b}, A₃, A₄, B₁, and B₂.^{5,6} In addition to these bioactive metabolites, we have also isolated esperamicin X (1), an inactive compound coproduced by the organism. Similarities in the physical properties of 1 with the bioactive metabolites have led us to undertake the structure elucidation of 1 (Figure 1).

Compound 1 was isolated as a white crystalline solid, mp 182–184 °C, $[\alpha]_D^{25} -36^\circ$ (*c* 0.5, CHCl₃). Its molecular formula was established as C₃₆H₄₀N₂O₁₄S by using FAB mass spectroscopy (MW 756) and elemental analysis. The IR spectrum of 1 had bands characteristic of hydroxyl, ester, amide, and enol ether functions.⁷ The UV spectrum of 1 was similar to that of esperamicin A₁.⁸ Examination of the ¹H and ¹³C NMR spectra of 1 showed the presence of numerous resonances observed in the spectrum of esperamicins A₁, A_{1b}, and A₂ and encouraged a more thorough analysis.⁹

(3) (a) Konishi, M.; Saitoh, K.; Ohkuma, H.; Kawaguchi, H. Japan Kokai 84-232 094, Dec 26, 1984. (b) Konishi, M.; Ohkuma, H.; Saitoh, K.; Kawaguchi, H.; Golik, J.; Dubay, G.; Groenewold, G.; Krishnan, B.; Doyle, T. W. *J. Antibiot.* 1985, 38, 1605–1609. (c) Kiyoto, S.; Nishikawa, M.; Terano, H.; Kohsaka, M.; Aoki, H.; Imanaha, H.; Kawai, Y.; Uchida, I.; Hashimoto, M. *J. Antibiot.* 1985, 38, 840–848. (d) Bunge, R. H.; Hurley, T. R.; Smitka, T. A.; Willmer, N. E.; Brankiewicz, A. J.; Steinman, C. E.; French, J. C. *J. Antibiot.* 1984, 37, 1566–1571. (e) Lee, M. D.; Greenstein, M.; Labeda, D. P. Eur. Patent Appl. 0 182 152, May 28, 1986.

(4) Esperamicins A₁, A_{1b}, and A₂ are active in a number of murine tumor models (P388, B16, M5076, etc.) at doses in the 100 ng/kg/injection range.⁶
(5) Manuscripts detailing the taxonomy and fermentation of BBM1675 are in preparation: Claridge, C. A.; Forenza, S.; Hatori, M.; Kawaguchi, H.; Kimball, D. L.; Lam, K. S.; Miyaki, T.; Titus, J. A.; Tomita, K.; Veitch, J. A., unpublished results, 1987.

(6) A manuscript detailing the isolation and biological activities of these components is in preparation: Bradner, W. T.; Forenza, S.; Golik, J.; Kawaguchi, H.; Konishi, M.; Matson, J. A.; Ohkuma, H.; Saitoh, K., unpublished results, 1987.

(7) IR bands at 3400, 2940, 1740 (sh), 1730, 1685, 1610, 1595, 1525, 1450, 1365, 1350, 1310, 1250, 1210, 1155, 1180, 1025, 1000, 785, 760, and 755 cm⁻¹.

(8) UV bands in methanol at λ_{max} (nm) 323 (ϵ 10900), 285 (ϵ 10500), and 253 (ϵ 25900).

(1) (a) Bristol-Myers Pharmaceutical Research and Development Division. (b) Cornell University. (c) Bristol-Myers Research Institute.

(2) The producing organism was collected at Pto Esperanza, Misiones, Argentina. Consequently we have given the trivial name of esperamicin to compounds isolated from the complex.

Methanolysis of **1** yielded the 2-deoxy-L-fucose derivative **2** identical in all respects with that obtained on methanolysis of esperamicins A₁ and A_{1b}^{3b} as well as a new product, **3**. Compound **3** was obtained as white crystals, mp 223 °C. The IR spectrum of **3** showed bands for ketone, urethane, and hydroxyl functions.¹⁰ The UV spectrum of **3** was uninformative with only very weak absorbances above 230 nm. A molecular formula of C₁₇H₁₇NO₆S (MW 363) was determined by high-resolution mass spectroscopy. From the ¹H and ¹³C NMR spectra, the presence of a number of substructural fragments could be deduced, i.e., a disubstituted aromatic ring, an allylic group =CHCH₂S, three isolated methine groups bearing heteroatoms, a ketone carbonyl, and two heteroatom substituted quaternary carbons.¹¹ Assignment of an unambiguous structure based on the data was not possible; consequently, crystals of **3** grown from methanol-chloroform were subjected to X-ray analysis.¹²

Figure 2 is a computer-generated perspective drawing of the final X-ray model. The X-ray experiment defined only the relative, not the absolute, stereochemistry. The tetracyclic core of the molecule can be dissected into smaller rings to discuss the conformation. There is a six-membered ring, atoms C1-C5 and C13, which is in a chair conformation. With respect to this ring, the sulfur substituent at C1 is equatorial, as are O5, O4, and N1. Substituents C6 and C12 are axial and form part of a cyclohexene ring—atoms C5, C6, C11, C12, C1, and C13. This ring is in the expected half-chair conformation; i.e., atoms C5, C6, C11, and C12 are planar with C13 above and C1 below this plane. The dihydrothiophene ring is planar with all torsional angles less than 2°. There is some bond lengthening around C1 which is indicative of strain.

It remained to establish the points of attachment of the 2-deoxy-L-fucose fragment to the core. The mass spectra of compounds **1** and **3** permit us to assign the point of attachment as being at C4. In the mass spectrum of **3**, major ions were observed at *m/z* 146 and 218. The exact mass of the *m/z* 146 ion establishes this fragment as C₅H₈NO₄. This corresponds to cleavage through bonds C1-C2 and C4-C5 with hydrogen transfer to this fragment. The fragment ion at *m/z* 218 is consistent with the aromatic side of this fragment without hydrogen transfer.¹³ Similarly in the EI mass spectrum of **1**, major fragmentation ions were observed at *m/z* 540 and 216. The *m/z* 540 ion is consistent

with the analogous C1-C2, C4-C5 cleavage in which the 2-deoxy-L-fucose chromophore is glycosidically attached to the C4 hydroxyl. The *m/z* 216 ion is consistent with the aromatic side of the fragment with hydrogen transfer. Attachment of the 2-deoxy-L-fucose at either C5 or C12 is inconsistent with the mass spectral fragmentation pattern of **1**. Further support for this assignment from ¹H and ¹³C NMR comparisons of **1** and **3** was available, e.g., the shift of the C4 carbon from δ 85.1 to 82.7 on going from **1** to **3** with a corresponding shift of the proton signal from δ 4.68 to 4.49. Little or no chemical shift differences for the C5 and C12 resonances were observed. The assignment of the α-glycosidic linkage in **1** was made on the basis of the C1'-H coupling constants to the C2' protons.

With the structure of esperamicin X (**1**) in hand, assignment of the NMR spectra data to specific structural features was accomplished. Comparison of the spectra of esperamicin X with those of esperamicin A₁ revealed numerous similarities between them, notably, the common presence of the 2-deoxy-L-fucose-aromatic chromophore, the allylic methylene attached to a heteroatom, the presence of the NHCO₂Me function, and the presence of the quaternary carbon at C5 (δ 77.3). A number of differences were also noted, especially the presence of the aromatic disubstituted ring and the quaternary carbon at 74.7 ppm in **1** and not in esperamicin A. Reconciliation of these structural similarities and differences between **1** and esperamicin A₁ is the subject of the following communication¹⁴ in this issue.

Registry No. 1, 107175-47-3; 2, 99407-56-4; 3, 107175-48-4.

Supplementary Material Available: Tables of fractional coordinates, thermal parameters, interatomic distances, interatomic angles, and torsional angles for **3** (4 pages). Ordering information is given on any current masthead page.

(14) Golik, J.; Dubay, G.; Groenewold, G.; Kawaguchi, H.; Konishi, M.; Krishnan, B.; Ohkuma, H.; Saitoh, K.; T. W. Doyle, J. Am. Chem. Soc., following paper in this issue.

Esperamicins, a Novel Class of Potent Antitumor Antibiotics. 3. Structures of Esperamicins A₁, A₂, and A_{1b}

Jerzy Golik,^{*1a} George Dubay,^{1a} Gary Groenewold,^{1a} Hiroshi Kawaguchi,^{1a} Masataka Konishi,^{1b} Bala Krishnan,^{1a} Hiroaki Ohkuma,^{1b} Kyo-ichiro Saitoh,^{1b} and Terrence W. Doyle^{1a}

Bristol-Myers Pharmaceutical
Research and Development Division
Wallingford, Connecticut 06492
Bristol-Myers Research Institute
Tokyo-Mequro, Tokyo, Japan
Received November 28, 1986

In the preceding communication in this issue, the structure elucidation of esperamicin X was described.² We now report the structure elucidations of esperamicins A₁, A₂, and A_{1b} (compounds **1a-c**, respectively, Figure 1) through chemical degradation and the analysis of the spectra of the degradation products. Esperamicin A₁ (**1a**) contains four sugars and an aromatic chromophore which are attached at two points to a bicyclic core. Of the four sugars in **1a**, three have not previously been reported. The central core contains a number of unique functionalities within a bicyclo[3.7.1] system; an allylic trisulfide attached to the bridging atom, a 1,5-dien-3-ene system, and an α,β-unsaturated ketone in

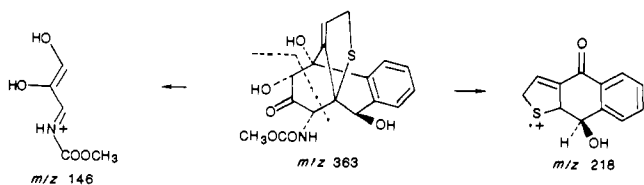
(9) The resonances attributable to the core are listed below. For those assigned to the 2-deoxy-L-fucose chromophore, see ref 3b: ¹H NMR of **1** (CD₃CN at 360 MHz) δ 7.71 (1 H, d, *J* = 7.5 Hz, C7-H), 7.27-7.41 (3 H, m, C8-H, C9-H, C10-H), 6.27 (1 H, t, *J* = 2.3 Hz, C14-H), 6.01 (1 H, br s, NH-CO₂Me), 5.21 (1 H, d, *J* = 9.9 Hz, C2-H), 4.68 (1 H, d, *J* = 2.3 Hz, C4-H), 4.48 (1 H, obsc, C12-H), 4.60 (1 H, s, C5-OH), 3.90 (2 H, m, obsc, C15-H₂), 3.65 (3 H, s, NHCO₂CH₃), and 3.59 (1 H, d, *J* = 2.9 Hz, C12-OH). ¹³C NMR of **1** (CD₃CN at 90 MHz) δ 74.4 (C1), 68.4 (C2), 201.2 (C3), 85.1 (C4), 76.4 (C5), 137.5 (C6), 128.2 (C7), 129.0 (C8), 129.1 (C9), 132.0 (C10), 135.5 (C11), 71.9 (C12), 142.2 (C13), 125.6 (C14), 38.9 (C15), 158.1 (CO₂Me), 53.1 (CO₂Me).

(10) IR bands at 3360, 3070, 2960, 2920, 2850, 2255, 1722, 1525, 1454, 1330, 1255, 1181, 1140, 1075, 1033, 910, 775, and 736 cm⁻¹.

(11) ¹H NMR of **3** (CD₃CN at 360 MHz) δ 7.49 (1 H, d, *J* = 8.1 Hz, C7-H), 7.23-7.35 (3 H, m, C8-H, C9-H, C10-H), 6.21 (1 H, t, *J* = 2.6 Hz, C14-H), 5.99 (1 H, br s, NHCO₂Me), 5.22 (1 H, d, *J* = 9.9 Hz, C2-H), 4.50 (1 H, obsc, C5-OH), 4.49 (1 H, obsc, C4-H), 4.48 (1 H, obsc, C12-H), 3.88 (2 H, m, C15-H₂), 3.62 (3 H, s, CO₂CH₃), 3.52 (1 H, d, *J* = 3.0 Hz, C12-OH), 3.36 (1 H, d, *J* = 5.1 Hz, C4-OH). ¹³C NMR of **3** (CD₃CN at 90 MHz) δ 74.6 (C1), 68.0 (C2), 202.6 (C3), 82.7 (C4), 77.3 (C5), 136.9 (C6), 127.9 (C7), 129.1 (C8), 129.1 (C9), 131.9 (C10), 135.4 (C11), 71.9 (C12), 142.0 (C13), 125.5 (C14), 39.0 (C15), 158.0 (NHCO₂Me), 53.2 (CO₂Me).

(12) Details of the X-ray determination are found in the supplementary material.

(13) Major ions in the mass spectrum of **3** have been confirmed by exact mass measurements.



(1) (a) Bristol-Myers Pharmaceutical Research and Development Division. (b) Bristol-Myers Research Institute.

(2) Golik, J.; Clardy, J.; Dubay, G.; Groenewold, G.; Kawaguchi, H.; Konishi, M.; Krishnan, B.; Ohkuma, H.; Saitoh, K.; Doyle, T. W. J. Am. Chem. Soc., preceding paper in this issue.